SUPPLEMENTARY INFORMATION

Asymmetric nucleosomes flank promoters in the budding yeast genome

Srinivas Ramachandran, Gabriel E. Zentner and Steven Henikoff

SUPPLEMENTAL FIGURE LEGENDS

Figure S1. Features of asymmetric nucleosomes. (A) A 10-kb snapshot of H4S47C-anchored cleavage mapping data. (B) The normalized frequency of left and right ends of the cleavage fragments averaged over nucleosome positions genome-wide is plotted. The left ends contribute to the -1 and +6 peaks around the dyad axis (left) and the right ends to contribute to the -6 and +1 peaks around the dyad axis (right).

Figure S2. Z-score difference distributions of asymmetric positions and all nucleosome positions. Distribution of the difference between the 5 ntd Z-score and the -2 ntd Z-score (top) highlights the cut-off of the 2.5 Z-score difference used to identify asymmetric nucleosomes, whereas the Z-score difference of most nucleosome positions is around zero. The distribution of difference between 5 ntd Z-score and 12 ntd Z-score (bottom) for asymmetric nucleosomes is significantly right-shifted from zero, indicating that for asymmetric nucleosomes, the 5 ntd Z-score is disproportionately higher than the 12 ntd Z-score, as expected for predominant cleavages by one H4 in the nucleosome rather than two H4s.

Figure S3. Distinction between centromeric nucleosomes and nucleosomes in the rest of the genome. (A) The normalized H4S47C-anchored cleavage frequency was averaged over the dyad axis for all nucleosomes and asymmetric nucleosomes and over the H4 position for centromeric nucleosomes. (B) The degree of asymmetry of all nucleosomes was compared to that of asymmetric nucleosomes and centromeric nucleosomes. The number inside the bar indicates the number of nucleosome positions that comprise each group. Error bars denote standard error of mean and the p-values were calculated using the Wilcoxon test.

Figure S4. Robustness of H4-S47C-anchored cleavage mapping. (A) The normalized cleavage frequency from three independent replicates are averaged over all yeast nucleosome positions and

plotted relative to the nucleosome dyad. (B) The normalized cleavage frequencies from three independent replicates are averaged over asymmetric nucleosome positions and is plotted relative to the nucleosome dyad axis. The nucleosomes are oriented so that the side of the dyad axis with more cleavages is on the right.

Figure S5. H4S47C-anchored cleavage data from *Brogaard et al.* (A) Heatmap of cleavage mapping data of 1500 symmetric nucleosomes (top), 1654 asymmetric nucleosomes with more cleavages on the left (middle) and 1585 asymmetric nucleosomes with more cleavages on the right side of the dyad (bottom), reproduced from Figure 1E. (B) Heatmap of cleavage mapping data of 1500 symmetric nucleosomes (top), 1654 asymmetric nucleosomes with more cleavages on the left (middle) and 1585 asymmetric nucleosomes with more cleavages on the right side of the dyad (bottom), plotted using data from the Short Read Archive (SRR438673-76) (Brogaard et al. 2012a).

Figure S6. H4-WT cleavage mapping. To confirm that the asymmetric cleavages we observed depended on the H4S47C mutation, we analyzed the cleavage frequency from an experiment where wild-type cells were labeled with 1, 10-orthophenanthroline and cleavage reactions were carried out in a manner identical to H4S47C-anchored cleavage mapping. In the experiment with the strain containing wild-type (WT) H4, we observe no specific cleavage positions at either asymmetric nucleosome positions or at all nucleosome positions.

Figure S7. Reproducible positional enrichment of asymmetric nucleosomes. Asymmetric nucleosome positions were independently identified in three replicate datasets and their enrichment at genic nucleosome positions and non-genic positions was calculated. p-values calculated using a hypergeometric test are shown for significantly enriched positions (+1 and -1).

Figure S8. H4S47C-anchored cleavage frequency at asymmetric ±1 nucleosome positions. (A) Heatmaps of cleavage mapping data at asymmetric +1 nucleosome positions plotted in the direction of

transcription. At a scale of dyad ±400 bp, the NDR and the downstream nucleosome array can be seen (left). At a scale of dyad ±15 bp, the asymmetric cleavages around the dyad are resolved (right). The nucleosome positions with higher cleavages downstream of the dyad (top) are separated from nucleosome positions with higher cleavages upstream of the dyad (bottom). (B) Same as (A) for asymmetric -1 nucleosome positions.

Figure S9. Turnover rate at asymmetric ±1 nucleosome positions. Box plots comparing the distribution of turnover Z-scores of all ±1 nucleosome positions and asymmetric ±1 nucleosome positions. The central line in the box-plot denotes the median, the upper and lower edges of the box denote the interquartile range and the whiskers extend to 1.5 times the interquartile range. Outliers are omitted for clarity.

Figure S10. MNase-seq as a probe of the accessibility of nucleosomal DNA. The distribution of MNase cuts, plotted relative to the nucleosome dyad axis for all +1 nucleosomes (n=4116) reveals peaks with a 10 bp periodicity, reflecting the accessibility of DNA wrapped around the histone octamer. The accessibility steadily decreases from the outer edge towards inside except at specific cuts ±5 bp of the dyad.

Figure S11. RSC binding does not depend on the direction of asymmetry. ChIP-seq of the RSC catalytic subunit, Sth1 is plotted for asymmetric nucleosomes that have higher cleavages on the downstream side of the dyad with respect to the TSS (n=171) and for asymmetric nucleosomes that have higher cleavages on the upstream side of the dyad with respect to the TSS (n=236). All nucleosomes are oriented towards the direction of transcription. The fragment centers were obtained from paired-end sequencing data and correspond to fragments of length 200 ± 20 bp. Data are averaged over a 20 bp moving window.

Figure S12. Nucleosome landscape after RSC depletion. Nucleosome landscape relative to the TSS is plotted for all genes with mapped ±1 nucleosome positions and genes with mapped asymmetric ±1 nucleosome positions. The data were obtained from a study in which Sth1 levels were depleted ~2 fold (Van de Vosse et al. 2013).

Figure S1

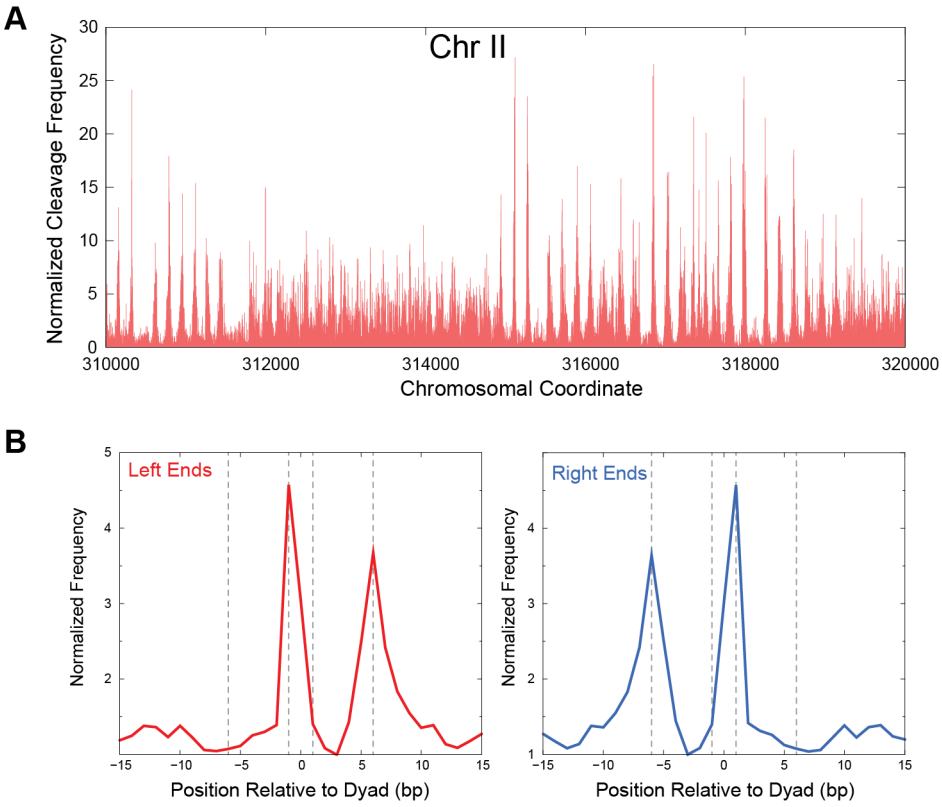
A
Chr II
Normalized Cleavage Frequency
30
25
20
15
10
5
0
310000
312000
314000
316000
318000
320000
Chromosomal Coordinate
B
Left Ends
Normalized Frequency
5
4
3
2
−15
−10
−5
0
5
10
15
Position Relative to Dyad (bp)
Right Ends
Normalized Frequency
4
3
2
1
−15
−10
−5
0
5
10
15
Position Relative to Dyad (bp)

Figure S2

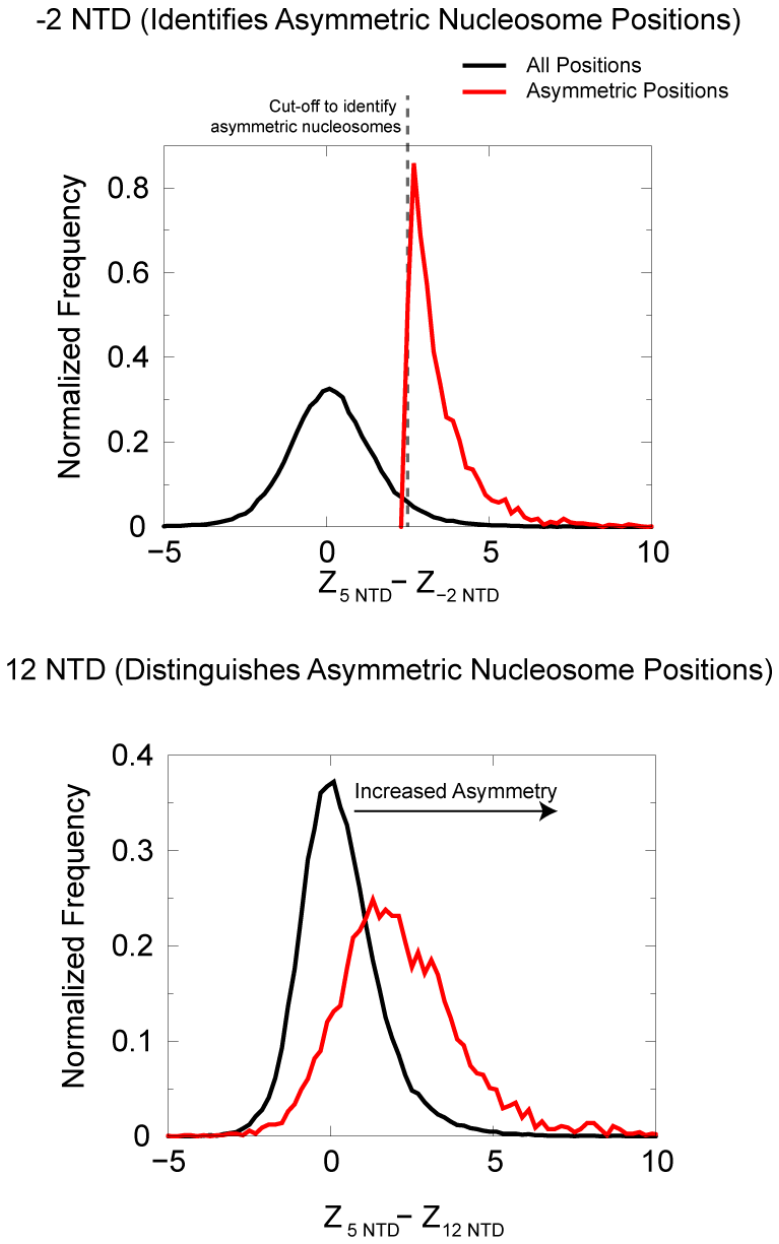
-2 NTD (Identifies Asymmetric Nucleosome Positions)
All Positions
Asymmetric Positions
Cut-off to identify asymmetric nucleosomes
Normalized Frequency
0.8
0.6
0.4
0.2
0
−5
0
5
10
Z 5 NTD − Z −2 NTD
12 NTD (Distinguishes Asymmetric Nucleosome Positions)
Increased Asymmetry
Normalized Frequency
0.4
0.3
0.2
0.1
0
−5
0
5
10
Z 5 NTD − Z 12 NTD

Figure S3

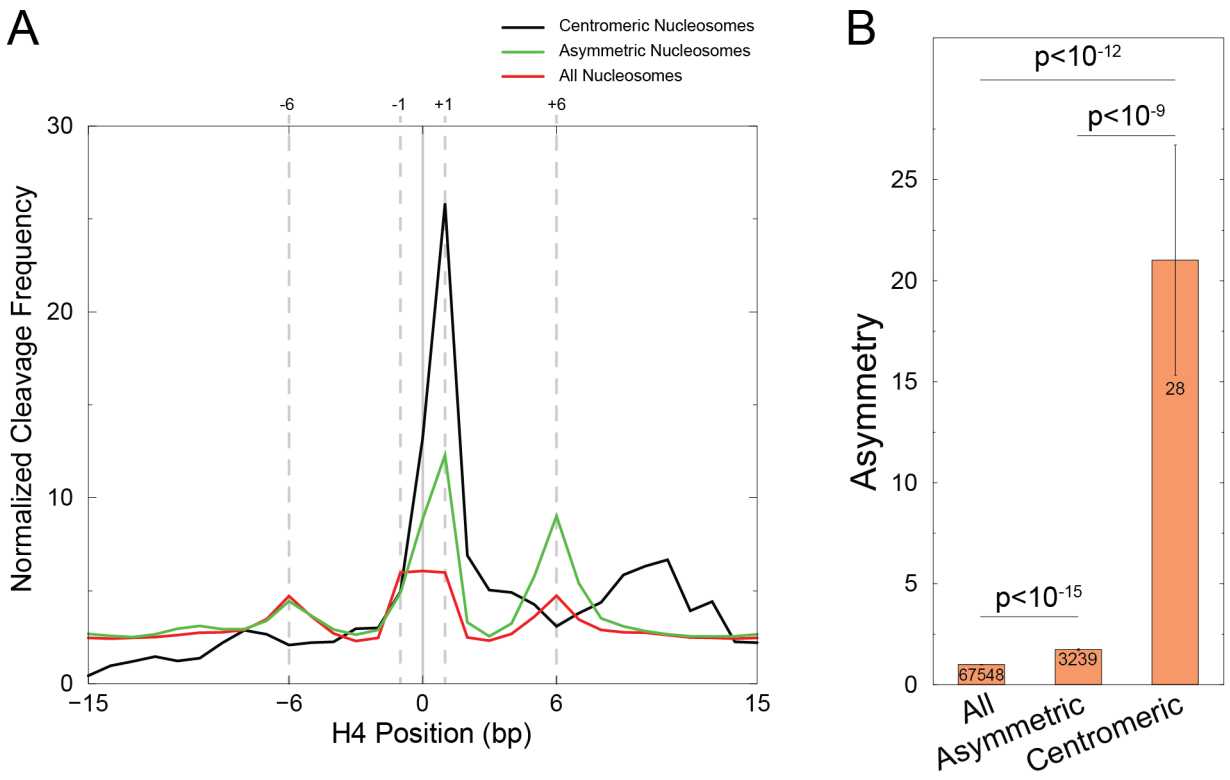
A
Centromeric Nucleosomes
Asymmetric Nucleosomes
All Nucleosomes
-6
-1
+1
+6
30
20
10
0
Normalized Cleavage Frequency
−15
−6
0
6
15
H4 Position (bp)
B
p<10-12
p<10-9
p<10-15
25
20
15
10
5
0
Asymmetry
28
67548
3239
All
Asymmetric
Centromeric

Figure S4

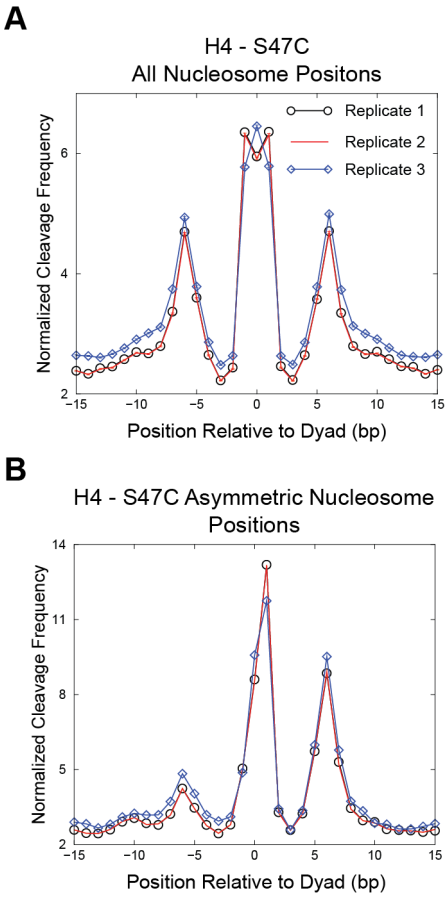
A
H4 - S47C
All Nucleosome Positons
Replicate 1
Replicate 2
Replicate 3
Normalized Cleavage Frequency
Position Relative to Dyad (bp)
B
H4 - S47C Asymmetric Nucleosome Positions
Normalized Cleavage Frequency
Position Relative to Dyad (bp)

Figure S5

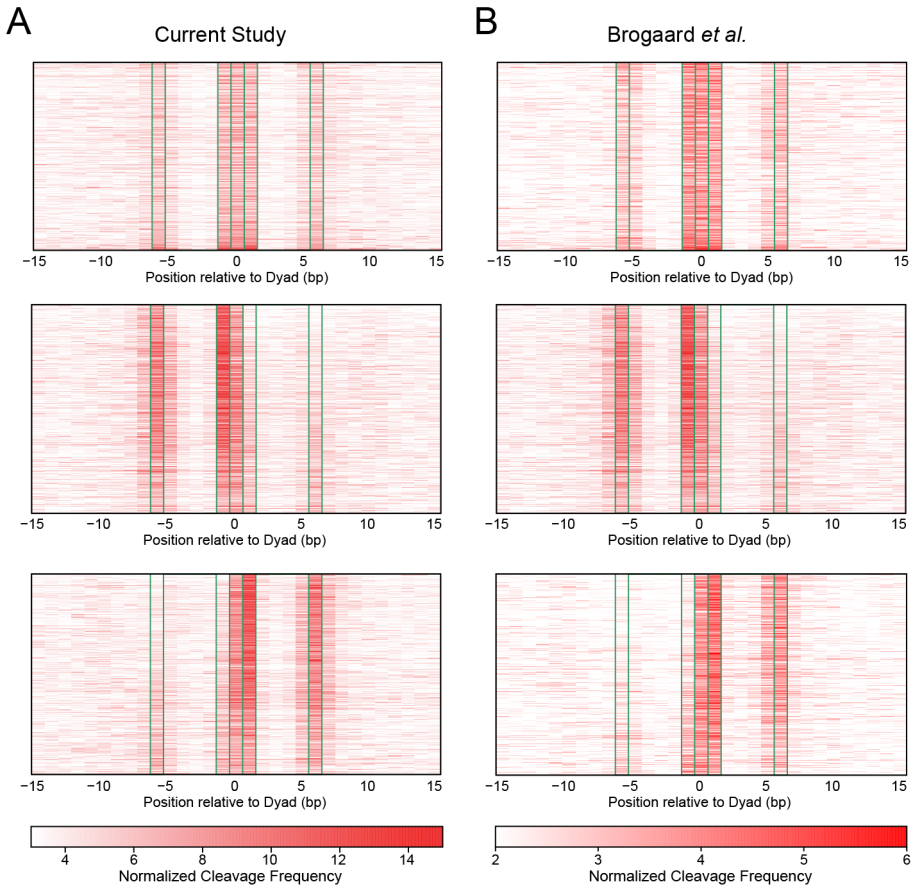
A
Current Study
B
Brogaard et al.
−15 −10 −5 0 5 10 15
Position relative to Dyad (bp)
4 6 8 10 12 14
Normalized Cleavage Frequency
2 3 4 5 6
Normalized Cleavage Frequency

Figure S6

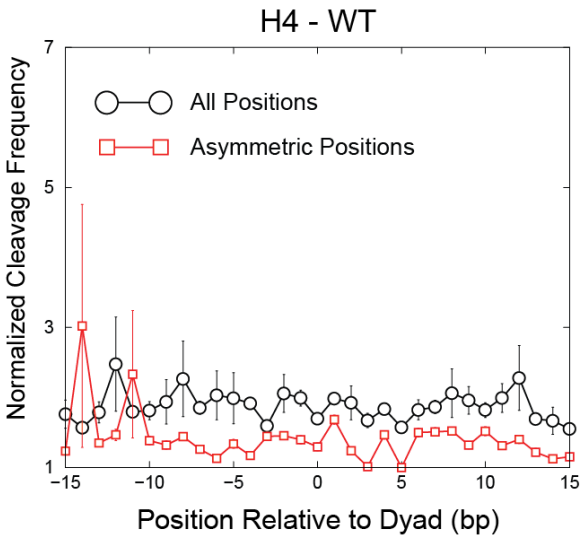
H4 - WT
All Positions
Asymmetric Positions
Normalized Cleavage Frequency
7
5
3
1
−15
−10
−5
0
5
10
15
Position Relative to Dyad (bp)

Figure S7

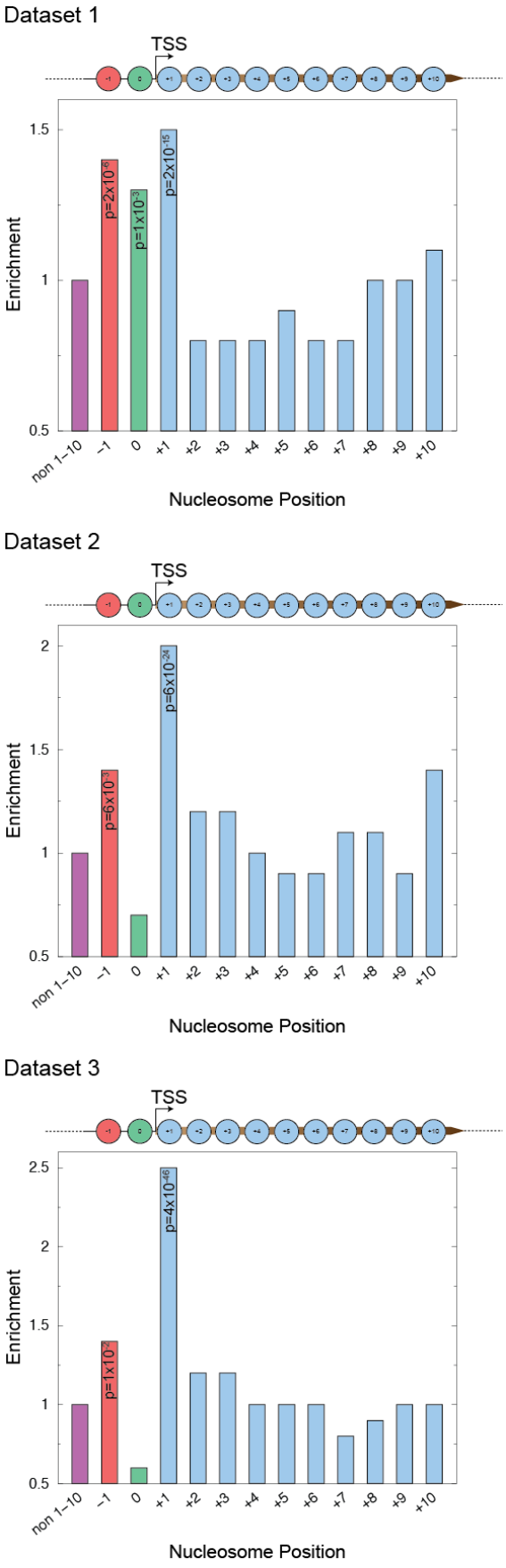
Dataset 1
TSS
Enrichment
1.5
1
0.5
p=2x10^-5
p=1x10^-3
p=2x10^-15
non 1–10
–1
0
+1
+2
+3
+4
+5
+6
+7
+8
+9
+10
Nucleosome Position
Dataset 2
TSS
Enrichment
2
1.5
1
0.5
p=6x10^-24
Nucleosome Position
Dataset 3
TSS
Enrichment
2.5
2
1.5
1
0.5
p=4x10^-46
Nucleosome Position

Figure S8

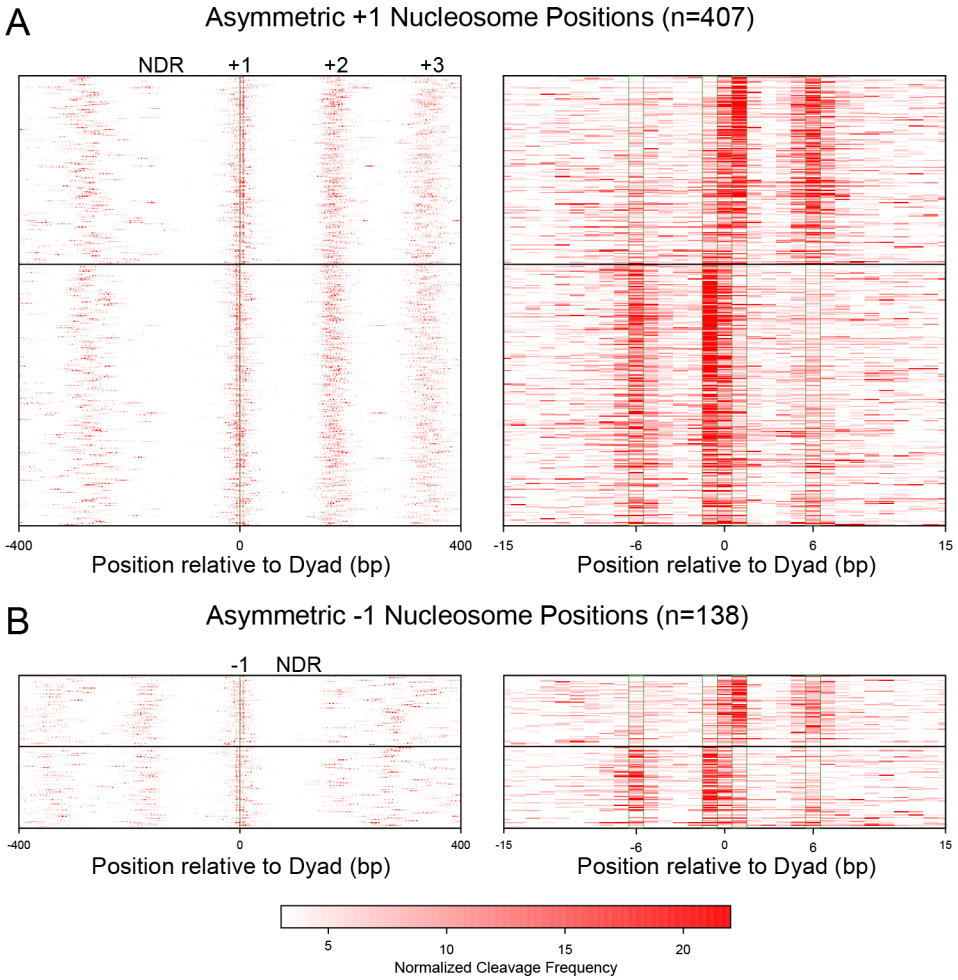
A
Asymmetric +1 Nucleosome Positions (n=407)
NDR
+1
+2
+3
-400
0
400
Position relative to Dyad (bp)
-15
-6
0
6
15
Position relative to Dyad (bp)
B
Asymmetric -1 Nucleosome Positions (n=138)
-1
NDR
-400
0
400
Position relative to Dyad (bp)
-15
-6
0
6
15
Position relative to Dyad (bp)
5
10
15
20
Normalized Cleavage Frequency

Figure S9

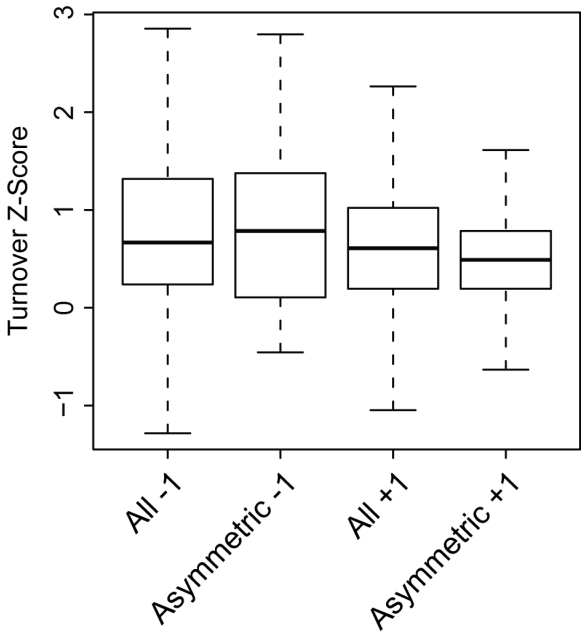

Figure S10

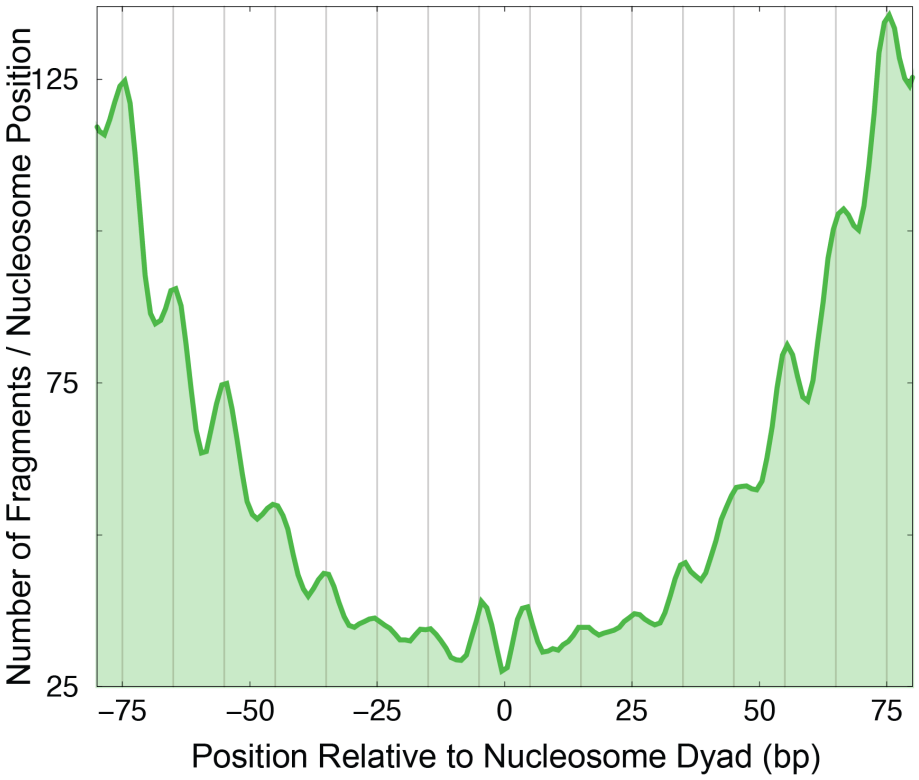
Number of Fragments / Nucleosome Position
125
75
25
−75
−50
−25
0
25
50
75
Position Relative to Nucleosome Dyad (bp)

Figure S11

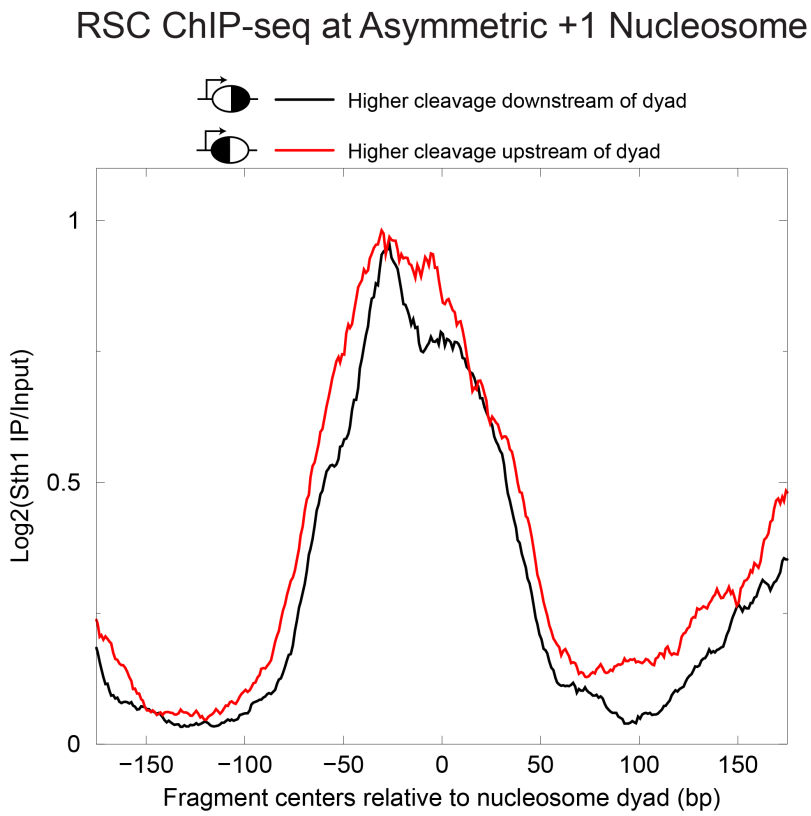
RSC ChIP-seq at Asymmetric +1 Nucleosome
Higher cleavage downstream of dyad
Higher cleavage upstream of dyad
Log2(Sth1 IP/Input)
1
0.5
0
−150
−100
−50
0
50
100
150
Fragment centers relative to nucleosome dyad (bp)

Figure S12

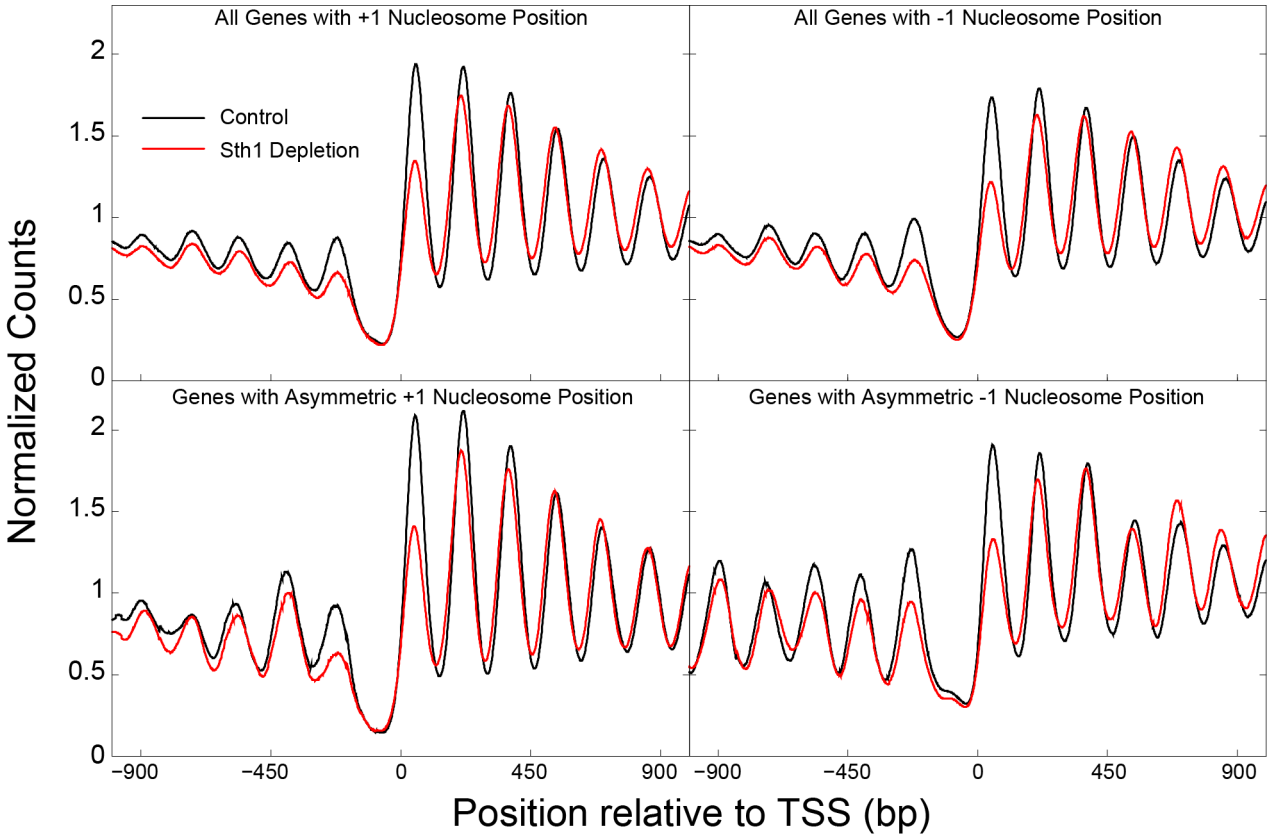
All Genes with +1 Nucleosome Position
All Genes with -1 Nucleosome Position
Genes with Asymmetric +1 Nucleosome Position
Genes with Asymmetric -1 Nucleosome Position
Control
Sth1 Depletion
Normalized Counts
Position relative to TSS (bp)
0
0.5
1
1.5
2
−900
−450
0
450
900

Table S1. Genes with asymmetric +1 nucleosome

YIL156W	YEL004W	YOR003W	YDL105W	YJL036W	YBL059C-A	YMR097C	YPR119W	YGR175C
YIL143C	YER010C	YOR036W	YDL102W	YJL019W	YBL031W	YMR104C	YPR134W	YGR185C
YIL129C	YER039C	YOR039W	YDL064W	YJL001W	YBL023C	YMR115W	YPR163C	YGR218W
YIL119C	YER041W	YOR064C	YDL058W	YJR010C-A	YBR002C	YMR123W	YPR186C	YGR227W
YIL084C	YER068W	YOR100C	YDL017W	YJR042W	YBR029C	YMR127C	YPR188C	YGR232W
YIL078W	YER069W	YOR106W	YDL013W	YJR053W	YBR044C	YMR128W	YPR193C	YGR245C
YIL076W	YER074W	YOR113W	YDL004W	YJR067C	YBR059C	YMR129W	YAL067C	YGR271C-A
YIL074C	YER114C	YOR117W	YDR005C	YJR083C	YBR076W	YMR152W	YAL048C	YGR277C
YIL072W	YER118C	YOR119C	YDR023W	YJR126C	YBR088C	YMR153W	YAL044C	
YIL051C	YER133W	YOR144C	YDR044W	YJR140C	YBR094W	YMR154C	YAL043C	
YIL019W	YER151C	YOR160W	YDR060W	YJR150C	YBR102C	YMR168C	YAL035W	
YIR012W	YER159C	YOR193W	YDR062W	YJR156C	YBR132C	YMR177W	YAL034C	
YIR034C	YER168C	YOR211C	YDR086C	YLL050C	YBR139W	YMR197C	YAL026C	
YCL054W	YNL307C	YOR213C	YDR103W	YLL040C	YBR147W	YMR220W	YAL025C	
YCL024W	YNL306W	YOR227W	YDR110W	YLL036C	YBR155W	YMR226C	YAL024C	
YCR003W	YNL284C	YOR253W	YDR145W	YLL014W	YBR160W	YMR229C	YAL017W	
YCR028C	YNL265C	YOR255W	YDR160W	YLL011W	YBR169C	YMR233W	YAL002W	
YCR030C	YNL262W	YOR305W	YDR163W	YLL001W	YBR170C	YMR235C	YAR014C	
YCR031C	YNL223W	YOR323C	YDR167W	YLR008C	YBR188C	YMR260C	YGL246C	
YCR032W	YNL202W	YOR346W	YDR190C	YLR014C	YBR205W	YMR270C	YGL243W	
YCR033W	YNL197C	YKL214C	YDR226W	YLR071C	YBR212W	YMR298W	YGL232W	
YCR035C	YNL147W	YKL204W	YDR235W	YLR087C	YBR216C	YPL266W	YGL227W	
YCR048W	YNL136W	YKL160W	YDR236C	YLR088W	YBR247C	YPL254W	YGL213C	
YCR071C	YNL135C	YKL154W	YDR244W	YLR102C	YBR248C	YPL234C	YGL212W	
YCR086W	YNL119W	YKL149C	YDR284C	YLR105C	YBR250W	YPL228W	YGL186C	
YCR092C	YNL101W	YKL126W	YDR292C	YLR117C	YBR268W	YPL214C	YGL180W	
YCR106W	YNL088W	YKL092C	YDR299W	YLR119W	YBR280C	YPL212C	YGL148W	
YHL023C	YNL087W	YKL058W	YDR301W	YLR127C	YBR282W	YPL202C	YGL137W	
YHL007C	YNL075W	YKL012W	YDR305C	YLR153C	YFL055W	YPL183C	YGL111W	
YHR004C	YNL054W	YKL010C	YDR315C	YLR183C	YFL037W	YPL175W	YGL106W	
YHR016C	YNL021W	YKL009W	YDR321W	YLR191W	YFL036W	YPL152W	YGL105W	
YHR038W	YNR007C	YKR001C	YDR323C	YLR193C	YFL009W	YPL133C	YGL093W	
YHR041C	YNR020C	YKR009C	YDR335W	YLR209C	YFL008W	YPL118W	YGL083W	
YHR076W	YNR031C	YKR028W	YDR337W	YLR213C	YFL002C	YPL115C	YGL077C	
YHR085W	YNR032C-A	YKR029C	YDR362C	YLR229C	YML118W	YPL105C	YGL060W	
YHR108W	YNR035C	YKR043C	YDR388W	YLR246W	YML105C	YPL070W	YGL054C	
YHR111W	YNR041C	YKR057W	YDR390C	YLR250W	YML104C	YPL059W	YGL027C	
YHR132C	YNR053C	YKR068C	YDR410C	YLR260W	YML086C	YPL031C	YGL026C	
YHR132W-A	YOL146W	YKR074W	YDR424C	YLR275W	YML081C-A	YPL023C	YGR043C	
YHR146W	YOL139C	YKR081C	YDR425W	YLR353W	YML073C	YPL009C	YGR085C	
YHR155W	YOL120C	YKR082W	YDR447C	YLR363C	YML068W	YPR020W	YGR090W	
YHR158C	YOL112W	YKR094C	YDR457W	YLR368W	YML064C	YPR062W	YGR100W	
YHR160C	YOL108C	YKR096W	YDR468C	YLR376C	YML060W	YPR081C	YGR101W	
YHR197W	YOL105C	YDL220C	YDR486C	YLR383W	YML046W	YPR083W	YGR116W	
YEL059C-A	YOL080C	YDL209C	YDR515W	YLR386W	YML043C	YPR085C	YGR128C	
YEL043W	YOL078W	YDL153C	YJL184W	YLR443W	YML041C	YPR098C	YGR132C	
YEL029C	YOL077C	YDL116W	YJL183W	YLR450W	YML032C	YPR102C	YGR133W	
YEL024W	YOL034W	YDL112W	YJL093C	YBL105C	YML029W	YPR112C	YGR141W	
YEL022W	YOL018C	YDL107W	YJL080C	YBL097W	YMR026C	YPR113W	YGR156W	
YEL012W		YDL106C	YJL072C	YBL076C	YMR061W	YPR115W	YGR170W	

Table S2. Genes with asymmetric -1 nucleosome

YIL140W	YKL082C	YBR228W
YIL033C	YKL068W	YBR240C
YIR021W	YKL024C	YFR021W
YCL035C	YKR003W	YFR051C
YCR034W	YKR009C	YML118W
YHR006W	YKR095W	YML111W
YHR052W	YDL245C	YML070W
YHR085W	YDL243C	YML019W
YHR094C	YDL176W	YMR017W
YHR142W	YDL168W	YMR146C
YEL069C	YDL035C	YMR208W
YEL062W	YDR019C	YMR260C
YER027C	YDR052C	YMR318C
YER052C	YDR110W	YPL282C
YER086W	YDR268W	YPL281C
YER090W	YDR294C	YPL266W
YER109C	YDR308C	YPL246C
YER183C	YDR414C	YPL188W
YNL327W	YDR446W	YPL169C
YNL322C	YDR499W	YPR054W
YNL312W	YJL190C	YPR194C
YNL297C	YJL186W	YAL067C
YNL254C	YJL154C	YAL025C
YNL222W	YJL129C	YAR033W
YNL189W	YJL093C	YGL258W
YNL185C	YJL083W	YGL251C
YNL166C	YJL014W	YGL223C
YNL142W	YJL005W	YGL170C
YNL076W	YJR055W	YGL139W
YNL032W	YJR110W	YGL137W
YNL026W	YJR158W	YGL040C
YNR020C	YLL064C	YGR010W
YNR039C	YLL063C	YGR140W
YNR059W	YLL018C	YGR200C
YNR072W	YLR013W	YGR206W
YOL136C	YLR025W	YGR252W
YOL124C	YLR027C	YGR257C
YOL022C	YLR047C	YGR271C-A
YOR001W	YLR166C	
YOR014W	YLR167W	
YOR061W	YLR222C	
YOR130C	YLR337C	
YOR281C	YLR418C	
YOR354C	YBL101C	
YOR393W	YBL080C	
YOR394W	YBL061C	
YKL192C	YBL059C-A	
YKL179C	YBL015W	
YKL134C	YBR070C	
YKL101W	YBR200W	

Table S3. GO term enrichment analysis of genes with asymmetric ±1 nucleosome

GOID	GO_term	Cluster frequency	Background frequency	P-value	FDR	Expected False Positives	Gene(s) annotated to the term
42255	ribosome assembly	19 out of 532 genes, 3.6%	54 out of 4355 background genes, 1.2%	0.014	0.00%	0.00	DRS2/YAL026C:FUN12/YAL035W:RPS14A/YCR031C:MAK21/YDR060W:RPS17B/YDR447C:SPB4/YFL002C:RPL11B/YGR085C:IPI1/YHR085W:RIX1/YHR197W:SQT1/YIR012W:MRT4/YKL009W:RPF2/YKR081C:RPL40B/YKR094C:RPS31/YLR167W:RPL6A/YML073C:BRX1/YOL077C:REX4/YOL080C:RPL11A/YPR102C:MRD1/YPR112C
70925	organelle assembly	30 out of 532 genes, 5.6%	114 out of 4355 background genes, 2.6%	0.036	0.00%	0.00	DRS2/YAL026C:FUN12/YAL035W:PKC1/YBL105C:KCC4/YCL024W:RPS14A/YCR031C:MAK21/YDR060W:RPS17B/YDR447C:NPR2/YEL062W:SPB4/YFL002C:ATG1/YGL180W:RPL11B/YGR085C:CBF2/YGR140W:STE20/YHL007C:NPR3/YHL023C:IPI1/YHR085W:RIX1/YHR197W:SQT1/YIR012W:MRT4/YKL009W:RPF2/YKR081C:RPL40B/YKR094C:RPS31/YLR167W:RPL6A/YML073C:CEP3/YMR168C:BNI5/YNL166C:ATG4/YNL223W:ATG3/YNR007C:BRX1/YOL077C:REX4/YOL080C:RPL11A/YPR102C:MRD1/YPR112C

GO Term enrichment carried out at www.yeastgenome.org; Gene set: Genes with asymmetric ±1 nucleosome positions (n=532); Background gene set: Genes with defined ±1 nucleosome positions (n=4355)

Table S4: P-values for enrichment of remodelers over input at asymmetric nucleosomes

Factor	Nucleosome Postion	T statistic	Paired T-test p-value (Null hypothesis: IP is less enriched relative to Input)	N
Chd1	Asymmetric +1	-7.1	1.000	407
Chd1	Asymmetric -1	0.4	0.358	137
Ino80	Asymmetric +1	-16.1	1.000	407
Ino80	Asymmetric -1	-2.5	0.992	137
Isw1	Asymmetric +1	-10.4	1.000	407
Isw1	Asymmetric -1	-5.3	1.000	137
Isw2	Asymmetric +1	-4.8	1.000	407
Isw2	Asymmetric -1	3.2	7E-04	137
Mot1	Asymmetric +1	-6.1	1.000	407
Mot1	Asymmetric -1	1.6	0.053	137
Swr1	Asymmetric +1	-0.1	0.542	399
Swr1	Asymmetric -1	0.7	0.230	134
RSC	Asymmetric +1	16.2	2E-46	407
RSC	Asymmetric -1	6.3	2E-09	137
Spt15	Asymmetric +1	1.4	0.077	407
Spt15	Asymmetric -1	3.0	0.002	138

Table S5: Strains used for native ChIP-seq

Factor Profiled	Strain Name	Genotype	Background	Source	Sample	Mapped Fragments
Ino80	YTT1728	*MATa ade2-1 can1-100 his3-11, 15 leu2-3, 112 trp1-1 ura3-1 RAD5+ INO80-3FLAG-kanMX4*	W1588-4C	Toshio Tsukiyama	Input	17200837
					ChIP	15244851
Swr1	GZY33	*MATa ade2-1 can1-100 his3-11, 15 leu2-3, 112 trp1-1 ura3-1 RAD5+ SWR1-3FLAG-kanMX4*	W1588-4C	G. E. Z.	Input	7179429
					ChIP	18369248
Sth1	GZY9	*MATa ade2-1 can1-100 his3-11, 15 leu2-3, 112 trp1-1 ura3-1 RAD5+ STH1-3FLAG-kanMX4*	W1588-4C	G. E. Z.	Input	33546327
					ChIP	16837779
Htz1	YTT3249	*MATα ade2-1 can1-100 his3-11, 15 leu2-3, 112 trp1-1 ura3-1 RAD5+ HTZ1-2L-3FLAG::KanMX*	W1588-4C	Toshio Tsukiyama	Input	44025854
					ChIP	12958113

Table S6: MNase-seq datasets

Published datasets – MNase-seq

Sample Number	Mapped Fragments	GEO Accession
1	28640945	GSM1080588
2	75234013	GSM968690
3	28864170	GSM968695
4	31312095	GSM968697
5	33069391	GSM968700
6	19821710	GSM1199785

Datasets generated in this study – MNase-seq

Sample Number	Mapped Fragments	Strain Name	Background	Genotype	Source
7	93646206	YTT1448	W1588-4C	*MATa ade2-1 can1-100 his3-11, 15 leu2-3, 112 trp1-1 ura3-1 RAD5+ ISW1-3FLAG-kanMX4*	Toshio Tsukiyama
8	17200837	YTT1728	W1588-4C	*MATa ade2-1 can1-100 his3-11, 15 leu2-3, 112 trp1-1 ura3-1 RAD5+ INO80-3FLAG-kanMX4*	Toshio Tsukiyama
9	7179429	GZY33	W1588-4C	*MATa ade2-1 can1-100 his3-11, 15 leu2-3, 112 trp1-1 ura3-1 RAD5+ SWR1-3FLAG-kanMX4*	G.E.Z.
10	21504106	GZY34	W1588-4C	*MATa ade2-1 can1-100 his3-11, 15 leu2-3, 112 trp1-1 ura3-1 RAD5+ FUN30-3FLAG-kanMX4*	G.E.Z.
11	28052211	YTT2094	W1588-4C	*MATa ade2-1 can1-100 his3-11, 15 leu2-3, 112 trp1-1 ura3-1 RAD5+ IOC3-3FLAG-kanMX4*	Toshio Tsukiyama
12	33546327	GZY9	W1588-4C	*MATa ade2-1 can1-100 his3-11, 15 leu2-3, 112 trp1-1 ura3-1 RAD5+ STH1-3FLAG-kanMX4*	G.E.Z.
13	59637061	YTT1448	W1588-4C	*MATa ade2-1 can1-100 his3-11, 15 leu2-3, 112 trp1-1 ura3-1 RAD5+ ISW1-3FLAG-kanMX4*	Toshio Tsukiyama
14	96429934	YTT1726	W1588-4C	*MATa ade2-1 can1-100 his3-11, 15 leu2-3, 112 trp1-1 ura3-1 RAD5+ CHD1-3FLAG-kanMX4*	Toshio Tsukiyama
Total Fragments			**574138435**		